Biochimica et Biophysica Acta, 687 (1982) 321–328
Elsevier Biomedical Press

BBA 71145

CALCIUM DOES NOT MEDIATE THE SHAPE CHANGE THAT FOLLOWS ATP DEPLETION IN HUMAN ERYTHROCYTES

JAMES E. FERRELL, Jr. and WRAY H. HUESTIS

Chemistry Department, Stanford University, Stanford, CA 94305 (U.S.A.)

(Received January 18th, 1982)

Key words: ATP depletion; Ca^{2+}; Crenation; Shape change; (Erythrocyte membrane)

Crenation, the shape change that follows ATP depletion in human erythrocytes, also follows ionphore-mediated Ca^{2+}-loading. Experiments designed to test whether Ca^{2+} mediates metabolic crenation showed that: (1) an influx of extracellular Ca^{2+} is not required for metabolic crenation; (2) metabolic crenation is accompanied by a 70% increase in $^{86}Rb^{+}$ permeability, a change much smaller than the increase expected if crenating concentrations of Ca^{2+} were released from bound intracellular pools; (3) A23187 plus EGTA, a treatment that depletes intracellular Ca^{2+} and stops Ca^{2+} crenation, does not affect metabolic crenation; (4) calmodulin inhibitors do not slow metabolic crenation. We conclude that Ca^{2+} does not mediate metabolic crenation. Albumin washes reverse Ca^{2+} crenation and partially reverse the early stages of metabolic crenation. We suggest that both Ca^{2+} crenation and metabolic crenation involve the accumulation of some amphiphilic species (e.g., lysolipid or diacylglycerol) in the cell membrane outer monolayer, and that ATP depletion induces a second crenating process which might be a reorganization of the cytoskeleton.

Introduction

When human erythrocytes are depleted of their ATP, a dramatic shape change ensues whereby biconcave discocytes are transformed into isovolumic spiculated echinocytes [1,2]. If the osmotic potential of hemoglobin is not opposed, the echinocytes swell, become spherocytes, and burst.

The role of ATP depletion in cell swelling and lysis is evident; cells accumulate salt and water, which they cannot pump out without ATP. In contrast, the link between ATP depletion and the attendant discocyte-echinocyte shape change (hereafter called metabolic crenation) is not clear. The hypothesis that expansion of the membrane outer monolayer or contraction of the inner monolayer turns discocytes into echinocytes [3] successfully explains the effects of many drugs on erythrocyte shape [4,5], but a relationship between monolayer areas and ATP levels is obscure.

Reports from many workers [6–11] have shown that ionophore-mediated Ca^{2+}-loading also causes a discocyte-to-echinocyte shape change. Under appropriate conditions this shape change can be resolved into two components: crenation (hereafter called Ca^{2+}-crenation) and cell shrinking. The latter phenomenon arises from the Gárdos effect [12,13], a Ca^{2+}-triggered increase in membrane potassium permeability. In low-K^{+} buffers, ionophore plus Ca^{2+} can cause a reversible conversion of discocytes to spherocytes without the appearance of many spiculated forms [12], whereas in high-K^{+} buffers the same treatment causes crenation without cell shrinking. Ca^{2+}-crenated cells are morphologically indistinguishable from metabolically crenated cells.

Abbreviation: EGTA, ethyleneglycol bis(β-aminoethyl ether)-*N*,*N*′-tetraacetic acid.

0005-2736/82/0000–0000/$02.75

The erythrocyte free Ca^{2+} concentration is maintained at about 100 nM to 1 μM by three factors: a membrane with low permeability to Ca^{2+}, cytoplasmic Ca^{2+} buffers, and a Ca^{2+} pump [14,15]. ATP may be involved in each of these aspects of Ca^{2+} regulation. First, ATP-depleted cells eventually show increased passive permeability to Ca^{2+} [16]. Second, ATP binds to Ca^{2+} and may be a significant Ca^{2+} buffer [17]. Third, ATP is the energy source for the Ca^{2+} pump [14,15]. Thus it is plausible that metabolic depletion could lead to increased intracellular Ca^{2+}. Early work showed this to be the case, although it was not clear that Ca^{2+} levels increased prior to metabolic crenation [18].

The roles of ATP in maintaining low intracellular Ca^{2+} and the similarities between metabolic and Ca^{2+} crenation led to the suggestion that a rise in intracellular Ca^{2+} levels mediates metabolic crenation [17–19]. The studies described here were undertaken to examine the role of Ca^{2+} in metabolic crenation of red cells.

Materials and Methods

All experiments were done using intact erythrocytes. Blood was obtained by venipuncture from adult volunteer donors. The red cells were separated by centrifugation and washed by one of two procedures. In the first, one volume of cells was thoroughly mixed with 4 vol. of cold 150 mM NaCl and centrifuged at 4°C for 5 min at 4000 $\times$ *g*. The supernatant, buffy coat, and top few milliliters of erythrocytes were aspirated and discarded. This procedure was repeated for a total of four washings, with the cells centrifuged for 10 min at 6000 $\times$ *g* following the final washing. The second washing procedure was employed when cells were to be treated with A23187. Cold 150 mM NaCl/100 μM EGTA (Sigma) was substituted for saline in the first three washes to ensure removal of extracellular calcium. Cells were usually used within 12 h of being drawn, and were always used within three days.

ATP depletion, restoration, and assay. Two different procedures were used to effect ATP depletion. For slow metabolic depletion, cells were incubated in capped plastic tubes at 37°C, hematocrit 20, with a buffer composed of 140 mM NaCl, 10 mM Tris-HCl, and 1 mM $MgSO_4$ (pH 7.2) plus penicillin G (100 μg/ml) and streptomycin (100 μg/ml) to retard bacterial growth. For fast metabolic depletion, the incubation buffer was supplemented with 10 mM glucose (Baker), 10 mM inosine (Sigma), 1 mM adenosine (Sigma), and 6 mM iodoacetamide (Sigma) [13].

Normal ATP levels were maintained or restored by incubating cells with buffer plus 10 mM glucose, 10 mM inosine, and 1 mM adenosine [13].

ATP levels in boiled extracts were measured by the luciferin-luciferase (Calbiochem-Behring) assay [20]. Excess EGTA was added to the boiled extracts to preclude inhibition of the assay by Ca^{2+} [18].

Ca^{2+}-loading and depleting. Ca^{2+}-loading or depleting was accomplished by incubating washed cells at 37°C, hematocrit 20, with A23187 (Calbiochem-Behring), a divalent cation ionophore. Ionophore A23187 was added in ethanol to yield final concentrations of 5 μM A23187 and 1% to 2.6% (v/v) ethanol. To prevent K^+ efflux and cell shrinking, which lead to alterations in cell lipid metabolism [21], we substituted KCl for NaCl in the incubation buffer. This substitution did not measurably change the rate of Ca^{2+}-loading or Ca^{2+}-crenation (cf. Refs. 12, 22). Solutions of $CaCl_2$ or EGTA were added as concentrates in buffer. Control cells were treated with an equal volume of ethanol. The efficacy of this procedure for Ca^{2+}-loading [10–13] or depleting [16] has been discussed in greater detail elsewhere.

$^{86}Rb^+$-loading and efflux. Washed cells were loaded with $^{86}Rb^+$ by incubation at 37°C, hematocrit 50, with NaCl/Tris/$MgSO_4$ buffer supplemented with sugars (glucose, inosine, and adenosine), EGTA (10–20 μM), and $^{86}RbCl$ (10 μCi/ml cells, spec. act. approx. 7 mCi/mg, New England Nuclear) for 24 h. The cells were pelleted and washed once with KCl/Tris/$MgSO_4$ buffer. In some experiments, the sugars were omitted to allow ATP to deplete during the $^{86}Rb^+$-loading.

$^{86}Rb^+$ efflux was measured by adding $^{86}Rb^+$-loaded cells to 4 vol. of KCl/Tris/$MgSO_4$ with or without Ca^{2+}, EGTA, A23187, sugars, and iodoacetamide. These suspensions were incubated in a shaking water bath at 37°C. At 10- or 15-min intervals, aliquots (200 μl) were added to 1 ml cold buffer, and centrifuged to pellet the cells. A 1-ml

aliquot of the supernatant was placed in a scintillation vial. Equilibrium ($t = \infty$) levels of $^{86}Rb^+$ were measured by mixing 200 μl of the hematocrit 20 suspensions with 1 ml buffer, and bleaching a 1 ml aliquot of this mixture with 1 ml 30% H_2O_2. Aquasol (New England Nuclear) scintillation fluid (10 ml) was added to each vial. The $^{86}Rb^+$ was quantified in a liquid scintillation counter, with the measured cpm corrected for decay. Quenching correction was unnecessary. The efflux was expressed as

$$\frac{^{86}Rb^+ \text{ in cells}}{^{86}Rb^+ \text{ in suspension}} = \frac{\text{cpm}(\infty) - \text{cpm}(t)}{\text{cpm}(\infty) - \text{cpm}(0)}$$

and was plotted logarithmically as a function of time.

Cell morphology assay. Cell shape was assayed by mixing 1 vol. of cell suspension, hematocrit 20, with 3 vols. of ice cold 1% glutaraldehyde (Sigma) in buffer, fixing the cells on ice for at least 45 min, and examining them by bright field microscopy at 400× magnification. One hundred cells were counted from each of three fields and classified as either echinocytes (echinocytes I–III and spheroechinocytes I and II, in the nomenclature of Bessis [23]) or as discocytes (discocytes plus probably some echinocytes I [23] (Fig. 1)). The percentage of echinocytes varied from field to field with a standard deviation of about 0–5% for samples with less than 15% or more than 85% echinocytes, and about 5–10% for samples with 15–85% echinocytes.

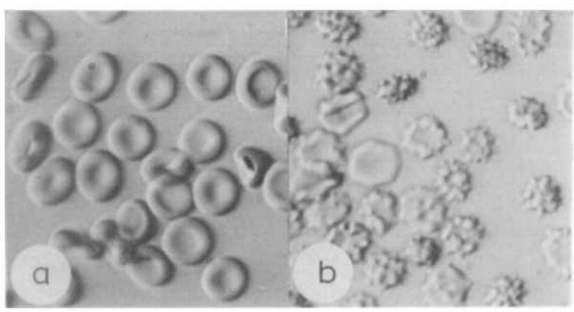

Fig. 1. Photomicrographs of (a) discocytes and (b) echinocytes produced by 31 h of slow metabolic depletion. The microscope used was a Nikon Labophot with a phase contrast condenser. To enhance the three dimensionality of the image, we centered the condenser and then 'clicked' it slightly out of the bright field position, resulting in oblique illumination.

Other materials. Trifluoperazine · 2 HCl (Smith, Kline and French) was provided by Dr. Dennis Smith. Gramicidin D (Sigma) was provided by Lawrence Weiss.

Results

Extracellular Ca^{2+} is not required for metabolic crenation

Washed erythrocytes were resuspended in buffer to allow slow metabolic depletion. ATP levels began at 1.1 ± 0.1 mmol/l packed cells and, after a lag of a few hours, fell exponentially with a first order rate constant of 0.24 h^{-1} (Fig. 2). The ATP depletion was largely due to the activity of the $(Na^+ + K^+)$-ATPase, and could be slowed greatly by substituting K^+ for Na^+ in the buffer. Crenation followed about 12 h behind ATP depletion. Neither ATP depletion nor the subsequent shape change was affected by substituting EGTA (1 mM) for Ca^{2+} (1 mM) in the incubation buffer.

Adding sugars and iodoacetamide accelerated ATP depletion about 15-fold. Metabolic crenation then lagged about 5 h behind ATP depletion. Once again, substituting EGTA (1 mM) for extracellular Ca^{2+} (100 μM) had no effect on the rate of ATP

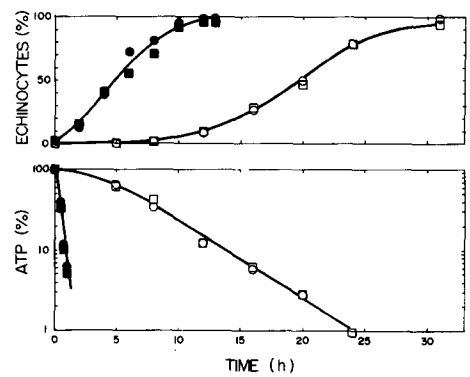

Fig. 2. Extracellular Ca^{2+} is not required for metabolic crenation. The percentages of echinocytes and ATP levels are shown for erythrocytes incubated at 37°C in NaCl buffer with (●,■) or without (○,□) glucose, adenosine, inosine, and iodoacetamide. The incubation buffers contained 1 mM Ca^{2+} (○); 100 μM Ca^{2+} (●); or 1 mM EGTA (■,□). At t=0, ATP levels were 1.1 ± 0.1 mmol/l packed cells. After a lag, ATP levels fell with first order rate constants of 3.7 h^{-1} (●,■) and 0.24 h^{-1} (○,□).

depletion or crenation (Fig. 2). Thus, any inward leak of Ca^{2+} is too small to be responsible for the crenation that follows fast or slow metabolic depletion. Similar results were reported by Feo and Mohandas [24] and by Sźasz et al. [17].

ATP depletion induces a small increase in $^{86}Rb^+$-permeability

Intracellular free Ca^{2+} levels could increase in the absence of extracellular Ca^{2+} if the ion were released from internal bound pools. Both ATP and 2,3-diphosphoglycerate bind Ca^{2+} with moderate affinity [18]. Unless some compensatory binding occurs in other intracellular Ca^{2+} buffers, metabolic ATP and 2,3-diphosphoglycerate depletion could liberate enough bound Ca^{2+} to trigger the shape change. One way to detect such an increase in free Ca^{2+} is to examine the efflux of K^+ (or $^{86}Rb^+$, a K^+ analog) from intact cells with normal or very low levels of ATP. Increases in intracellular Ca^{2+}, perhaps to as little as 300 nM [25,26], cause an increase in erythrocyte membrane K^+ permeability (the Gárdos effect [12]). $^{86}Rb^+$ efflux was measured in cells treated with iodoacetamide and in control cells. As shown in Fig. 3a, $^{86}Rb^+$ efflux was slightly slower in the iodoacetamide-treated cells than in control cells. The opposite result would be expected if metabolic depletion freed significant amounts of Ca^{2+}. Suspecting that iodoacetamide might inhibit some component of the 'Gárdos protein', we repeated the experiment without iodoacetamide. Cells were simultaneously loaded with $^{86}Rb^+$ and metabolically depleted by the slow procedure. To one aliquot of these cells, sugars were added to restore ATP levels and discoid cell shape. As shown in Fig. 3b, the ATP-depleted cells showed about 70% faster $^{86}Rb^+$ efflux than the control cells. This acceleration could reflect an increase in intracellular Ca^{2+}.

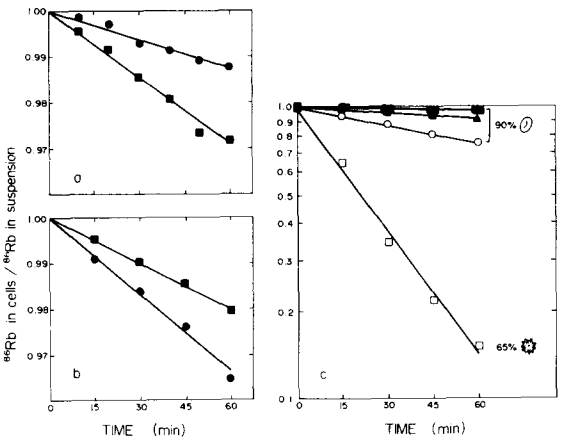

Fig. 3. $^{86}Rb^+$ efflux in metabolically depleted cells and Ca^{2+}-loaded cells. (a) Erythrocytes were loaded with $^{86}Rb^+$. $^{86}Rb^+$ efflux was then measured in KCl buffer supplemented with glucose, inosine, and adenosine with (●) or without (■) iodoacetamide. First order rate constants for $^{86}Rb^+$ efflux were 0.030 h^{-1} (■) and 0.013 h^{-1} (●). (b) After $^{86}Rb^+$ loading and slow metabolic depletion, erythrocytes were incubated for 7 h with (■) or without (●) glucose, inosine, and adenosine. Morphology was 100% discocytes (■) and 97% echinocytes (●). First order rate constants for $^{86}Rb^+$ efflux were then measured to be 0.021 h^{-1} (■) and 0.035 h^{-1} (●). (c) Erythrocytes were loaded with $^{86}Rb^+$. $^{86}Rb^+$ efflux was then measured in KCl buffer supplemented with glucose, inosine, and adenosine (●, $k=0.029$ h^{-1}) plus A23187 and 1 mM EGTA (■, $k=0.025$ h^{-1}), 1 μM Ca^{2+} (▲, $k=0.086$ h^{-1}), 10 μM Ca^{2+} (○, $k=0.29$ h^{-1}) or 100 μM Ca^{2+} (□, $k=1.9$ h^{-1}). At $t=60$ min, all samples were 90% discocytes except for (□), which contained 65% echinocytes.

To see if this free Ca^{2+} level was sufficient to cause crenation, we measured $^{86}Rb^+$ efflux and cell morphology while incubating cells with A23187 and several concentrations of Ca^{2+}. As shown in Fig. 3c, A23187 plus EGTA caused no increase in $^{86}Rb^+$ efflux over the control rate. When EGTA was replaced by 1 and 10 μM Ca^{2+}, $^{86}Rb^+$ efflux increased 3- and 10-fold respectively; however, no crenation was observed. Therefore, the small acceleration of $^{86}Rb^+$ efflux in metabolically depleted cells (Fig. 3b) corresponds to an increase in free intracellular Ca^{2+} insufficient to induce crenation. When cells were incubated with A23187 and 100 μM Ca^{2+}, both Ca^{2+} crenation and a 66-fold rise in $^{86}Rb^+$ permeability occurred (Fig. 3c).

A23187 plus EGTA halts Ca^{2+} crenation but not metabolic crenation

Erythrocytes were incubated with A23187 and 100 μM Ca^{2+} in KCl buffer with glucose, inosine, and adenosine. At 10-min intervals the Ca^{2+} loading was reversed by adding 500 μl of the suspension to 1 ml of buffer containing 1 mM EGTA. As shown in Fig. 4, EGTA treatment stopped but did not reverse the shape change. Treating metabolically depleted cells with A23187 and EGTA did not alter the rate of crenation (Fig. 5).

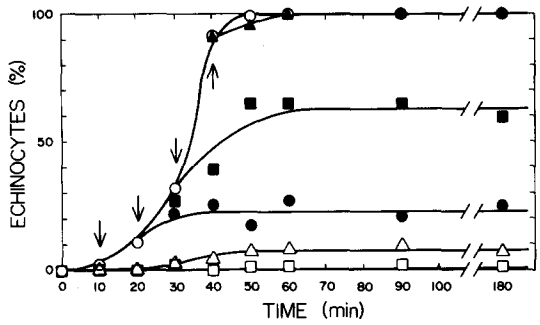

Fig. 4. EGTA halts Ca^{2+} crenation. Erythrocytes were incubated at 37°C with 5 μM A23187 and 100 μM Ca^{2+} in KCl buffer with glucose, inosine, and adenosine (○). Aliquots of this suspension were added to 2 vol. of buffer containing 1 mM EGTA at $t=0$ (□), 10 min (△), 20 min (●), 30 min (■), or 40 min (▲).

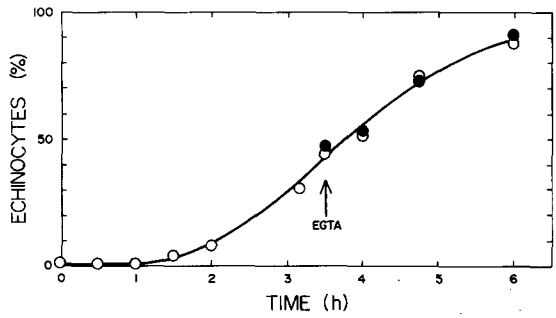

Fig. 5. EGTA does not affect metabolic crenation. Erythrocytes were incubated at 37°C in KCl buffer supplemented with iodoacetamide, glucose, inosine, and adenosine (○). At $t=3.5$ h, an aliquot of the suspension was added to 1 vol. of buffer containing 5 μM A23187 and 1 mM EGTA (●).

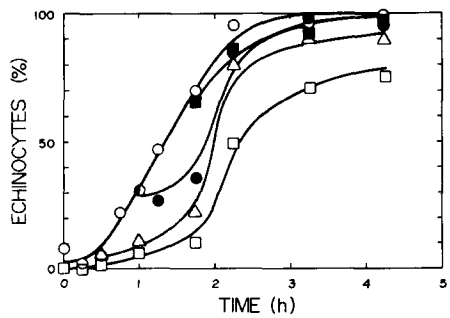

Fig. 6. EGTA slows Ca^{2+} crenation but not metabolic crenation. Erythrocytes were metabolically depleted by 15 min of incubation at 37°C in KCl buffer with iodoacetamide, glucose, inosine, and adenosine. At $t=0$, 5 μM A23187 and 100 μM Ca^{2+} were added to begin Ca^{2+} loading (○). Aliquots were taken and added to 1 vol. of the same buffer plus 1 mM EGTA at $t=0$ (□), 30 min (△), 45 min (●), or 105 min (■).

The experiment shown in Fig. 4 was repeated using cells metabolically depleted with iodoacetamide before Ca^{2+}-loading. EGTA treatments slowed the shape change until, at about $t=2$ h, all of the EGTA-treated cells crenated (Fig. 6). This time interval is typical of the lag between iodoacetamide treatment and metabolic crenation in cells treated with an equal volume of ethanol. A reasonable interpretation is that EGTA halted the rapid Ca^{2+} crenation but did not influence the slower metabolic crenation.

Albumin washes reverse Ca^{2+} crenation and partially reverse metabolic crenation

Erythrocytes were incubated with A23187 and 100 μM Ca^{2+} in KCl buffer. At 15-min intervals, aliquots of cells were washed first with 6 vol of KCl buffer plus 1% bovine serum albumin (w/v) and then with 30 vol. of KCl buffer. Albumin removes A23187 and outer monolayer lysolipid from erythrocytes but does not affect the morphology of discocytes or of end-stage echinocytes produced by metabolic depletion [27,28]. The albumin-washed cells were resuspended in KCl buffer. As shown in Fig. 7, this washing procedure partially reversed the Ca^{2+} crenation. When the incubation buffer contained glucose, inosine, and adenosine, the reversal was nearly complete and resulted in the formation of stomatocytes as well as discocytes (Fig. 8). These discocytes were noticeably smaller than untreated discocytes. Early

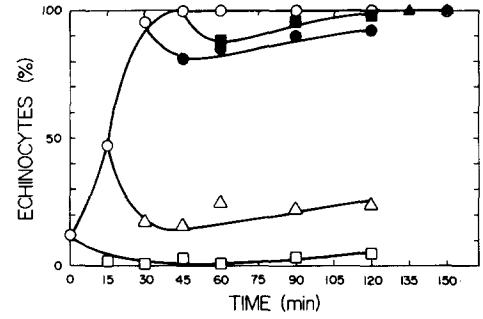

Fig. 7. Effect of albumin washes on Ca^{2+} crenation. Erythrocytes were incubated at 37°C in KCl buffer with 5 μM A23187 and 100 μM Ca^{2+} (○). Aliquots were washed first with 6 vol. of KCl buffer plus 1% bovine serum albumin and then with 30 vol. of KCl buffer plus 1% bovine serum albumin and the with 30 vol. of KCl buffer at $t=0$ (□), 15 min (△), 30 min (●), 45 min (■), or 120 min (▲).

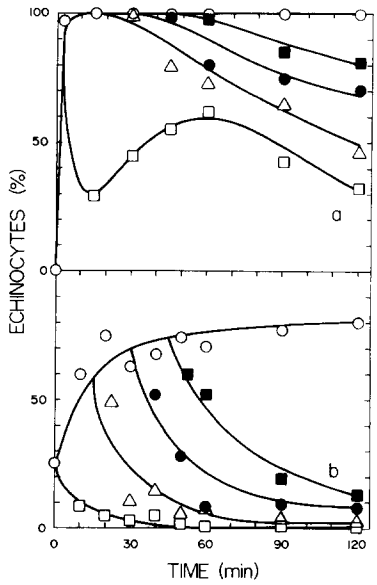

Fig. 8. Albumin washes reverse Ca^{2+} crenation. Erythrocytes were incubated at 37°C in KCl buffer containing glucose, inosine, adenosine, 100 μM Ca^{2+}, and 10 μM A23187 (a) or 5 μM A23187 (b). Aliquots were washed with bovine serum albumin as described for Fig. 7.

stages of metabolic crenation also were partially reversed by adding albumin, but later stages were unaffected (Fig. 9). Control experiments showed that metabolic crenation was not affected by washing with buffers containing no albumin.

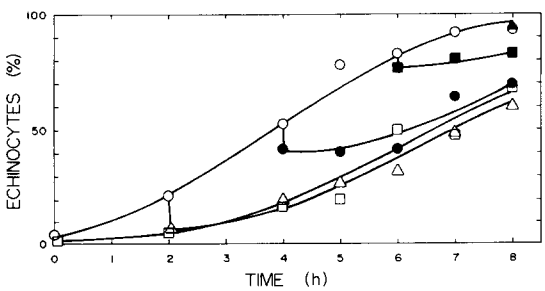

Fig. 9. Albumin washed partially reverse metabolic crenation. Erythrocytes were incubated at 37°C in NaCl buffer containing iodoacetamide, glucose, inosine, and adenosine (○). Aliquots were taken and added to 1 vol. of the same buffer plus 1% bovine serum albumin at $t=0$ (□), 2 h (△), 4 h (●), 6 h (■), and 8 h (▲). Similar results were obtained using the albumin washing method described for Fig. 7.

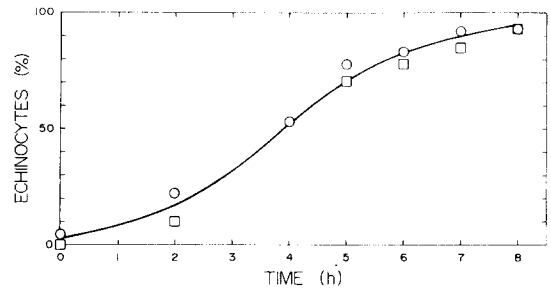

Fig. 10. Metabolic crenation is not inhibited by trifluoperazine. Erythrocytes were incubated at 37°C with NaCl buffer containing iodoacetamide, glucose, inosine, and adenosine in the presence (□) and absence (○) of the calmodulin inhibitor trifluoperazine (25 μM).

Calmodulin inhibitors do not retard metabolic crenation

The possible role of a calmodulin-Ca^{2+} complex in metabolic crenation was examined using the calmodulin inhibitors trifluoperazine and chlorpromazine [28]. Erythrocytes were incubated with 25 μM trifluoperazine in NaCl buffer containing adenosine, inosine, glucose, and iodoacetamide. Because it is an inner monolayer intercalator [4], trifluoperazine eliminated the small population of echinocytes often seen at early time points and transformed some discocytes into stomatocytes. After 2 h incubation the stomatocytes had disappeared. Crenation of the trifluoperazine-treated cells then lagged only slightly behind crenation of control cells (Fig. 10). Similar results were obtained with trifluoperazine (25 μM) or chlorpromazine (50 μM) in the absence of adenosine, inosine, glucose, and iodoacetamide (data not shown).

Discussion

Calcium-loading and ATP depletion have similar effects on red cell morphology which suggests that Ca^{2+} might mediate metabolic crenation. Two additional criteria must be satisfied to establish Ca^{2+} as mediator of this process. First, an appropriate increase in free intracellular Ca^{2+} must accompany metabolic crenation. We found no evidence for such an increase. Extracellular Ca^{2+} was not required for metabolic crenation (Fig. 2) and any increase in free intracellular Ca^{2+} was insuffi-

cient to trigger a large Gárdos potassium efflux, and thus was insufficient to induce crenation (Fig. 3). Second, depletion of intracellular Ca^{2+} must inhibit metabolic crenation. Intracellular Ca^{2+} was depleted by adding EGTA to the suspension buffer of A23187-treated cells. This treatment halted Ca^{2+} crenation but not metabolic crenation (Figs. 4–6). We conclude from these findings that Ca^{2+} does not mediate metabolic crenation.

Several studies have suggested ways that increases in Ca^{2+} or decreases in ATP could alter erythrocyte shape and deformability. Some of these mechanisms involve alterations in membrane lipid composition. Both Ca^{2+}-loading and ATP depletion lead to increases in membrane 1,2-diacylglycerol levels [29–33]. Ca^{2+}-loading stimulates the formation of lysolipid [34] and phosphatidic acid [31], as well as the degradation of phosphatidylinositol polyphosphates [35,36]. Moreover, increased Ca^{2+} levels could allow acidic inner monolayer phospholipids to pack more tightly. Such changes in cell lipid composition or packing could disrupt the membrane 'bilayer balance', with a relative expansion of the outer monolayer leading to crenation [3].

Changes in Ca^{2+} or ATP levels could also affect cell shape by altering the organization of the cytoskeleton, which is composed largely of spectrin, actin, and bands 4.1 and 4.9. In intact cells, small changes (100 nM to 10 μM) in Ca^{2+} concentration alter the rate of spectrin phosphorylation [37]. In vitro, physiological concentrations of Ca^{2+}, ATP, and 2,3-diphosphoglycerate dissociate crude mixtures of cytoskeletal proteins [38,39].

The results shown in Figs. 6–8 comment on possible mechanisms for Ca^{2+} crenation. EGTA plus A23187 rapidly depletes cells of Ca^{2+}; albumin removes A23187, allowing cells to pump out Ca^{2+} as long as ATP is not depleted. If Ca^{2+} per se causes crenation, then either protocol should restore the normal biconcave shape. However, A23187 plus EGTA only halted crenation, and albumin induced the formation of stomatocytes as well as discocytes, particularly when end-stage Ca^{2+}-crenated cells were washed. Perhaps Ca^{2+} stimulates the formation of an abnormal lipid (e.g. lysolipid or diacylglycerol) that expands the outer monolayer more than the inner monolayer. When albumin removes the A23187 it could also remove abnormal outer monolayer lipids, and abnormal lipid remaining in the inner monolayer could convert the cells to stomatocytes.

The reversal of early stages of metabolic crenation by albumin (Fig. 9) also points to possible production of an abnormal lipid. In contrast, end-stage ATP-depleted echinocytes are not affected by albumin washes. These findings show that metabolic crenation involves a second process, perhaps a reorganization of the cytoskeleton, that can be reversed by restoring ATP levels but not by albumin washes.

Acknowledgements

We thank Dr. Christina Harbury, Division of Hematology, Department of Medicine, Stanford University School of Medicine, for supplying some of the erythrocytes used in this work. This work was supported by the National Institutes of Health (HL23787 and HL00258) and by the American Heart Association (80 990).

References

1 Nakao, M., Nakao, T. and Yamazoe, S. (1960) Nature 187, 945–946
2 Nakao, M., Nakao, T. Yamazoe, S. and Yoshikawa, H. (1961) J. Biochem. 49, 487–492
3 Sheetz, M.P. and Singer, S.J. (1974) Proc. Natl. Acad. Sci. U.S.A. 71, 4457–4461
4 Fujii, T., Takashi, S., Tamura, A., Motoko, W. and Kanaho, Y. (1979) Biochem. Pharmacol. 28, 613–620
5 Matayoshi, E.D. (1980) Biochemistry 19, 3414–3422
6 Dunn, M.J. (1974) Biochim. Biophys. Acta 352, 97–116
7 Palek, J., Stewart, G. and Lionetti, F.J. (1974) Blood 44, 583–597
8 White, J.G. (1974) Am. J. Pathol. 77, 507–518
9 Kirkpatrick, F.H., Hillman, D.G. and LaCelle, P.L. (1975) Experientia 31, 653–654
10 Kuettner, J.F., Dreher, K.L., Rao, G.H.R., Eaton, J.W., Blackshear, P.L. and White, J.G. (1977) Am. J. Pathol. 88, 81–94
11 Lake, W., Rasmussen, H. and Goodman, D.B.P. (1977) J. Membrane Biol. 32, 93–113
12 Sarkadi, B., Sźasz, I. and Gárdos, G. (1976) J. Membrane Biol. 26, 357–370
13 Lew, V.L. and Ferreira, H.G. (1978) in Current Topics in Membranes and Transport (Bronner, F. and Kleinzeller, A., eds.), Vol. 10, pp. 217–277, Academic Press, New York
14 Schatzmann, H.J. and Bürgin, H. (1978) Ann. N.Y. Acad. Sci. 307, 125–147

15 Sarkadi, B. (1980) Biochim. Biophys. Acta 604, 159–190
16 Ferreira, H.G. and Lew, V.L. (1977) in Membrane Transport in Red Cells (Ellory, J.C. and Lew, V.L., eds.), pp. 53–91, Academic Press, New York
17 Szász, I., Teitel, P. and Gárdos, G. (1970) Acta Biochim. Biophys. Acad. Sci. Hung. 5, 409–413
18 Edmondson, J.W. and Li, T.-K. (1976) Biochim. Biophys. Acta 443, 106–113
19 Weed, R.I., LaCelle, P.L. and Merrill, E.W. (1969) J. Clin. Invest. 48, 795–809
20 Kimmich, G.A., Randles, J. and Brand, J.S. (1975) Anal. Biochem. 69, 187–206
21 Dise, C.A., Goodman, D.B.P. and Rasmussen, H. (1980) J. Biol. Chem. 255, 5201–5207
22 Dreher, K.L., Eaton, J.W., Breslawec, K.P., Berger, E., Blackshear, P.L. and White. J.G. (1980) Am. J. Pathol. 101, 543–556
23 Bessis, M. (1973) in Red Cell Shape (Bessis, M., Weed, R.I. and Leblond, P.F., eds.), pp. 1–24, Springer-Verlag, New York
24 Feo, C. and Mohandas, N. (1977) Nature 265, 166–168
25 Simons, T.J.B. (1976) J. Physiol. 256, 209–225
26 Simons, T.J.B. (1976) J. Physiol. 256, 227–244
27 Sheetz, M.P., Painter, R.G. and Singer, S.J. (1976) J. Cell Biol. 70, 193–203
28 T. Sato (1973) Chem. Pharm. Bull. 21, 176–183
29 Wolff, D.J. and Brostrom, C.O. (1979) Adv. Cyclic Nucleotide Res. 11, 27–88
30 Allan, D. and Michell, R.H. (1975) Nature 258, 348–349
31 Allan, D., Billah, M.M., Finean, J.B. and Michell, R.H. (1976) Nature 261, 58–60
32 Allan, D., Watts, R. and Michell, R.H. (1976) Biochem. J. 156, 225–232
33 Allan, D. and Michell, R.H. (1976) Biochim. Biophys. Acta 455, 824–830
34 Allan, D. and Michell, R.H. (1977) Biochem. J. 166, 495–499
35 Shohet, S.B. and Haley, J.E. (1973) in Red Cell Shape (Bessis, M., Weed, R.I. and Leblond, P.F., eds.), pp. 41–58, Springer-Verlag, New York
36 Allan, D. and Michell, R.H. (1978) Biochim. Biophys. Acta 508, 277–286
37 Quist, E.E. and Reece, K.L. (1980) Biochem. Biophys. Res. Commun. 95, 1023–1030
38 Nelson, M.J. and Huestis, W.H. (1980) Biochim. Biophys. Acta 600, 398–405
39 Fowler, V. and Taylor, D.L. (1980) J. Cell Biol. 85, 361–376
40 Sheetz, M.P. and Casaly, J. (1980) J. Biol. Chem. 255, 9955–9960